

Quantum dynamics of an Ising spin chain in a random transverse field

Xun Jia and Sudip Chakravarty*

Department of Physics and Astronomy, University of California Los Angeles, Los Angeles, California 90095-1547, USA

(Received 27 July 2006; revised manuscript received 31 August 2006; published 30 November 2006)

We consider an Ising spin chain in a random transverse magnetic field and compute the zero temperature wave vector and frequency dependent dynamic structure factor numerically by using Jordan-Wigner transformation. Two types of distributions of magnetic fields are introduced. For a rectangular distribution, a dispersing branch is observed, and disorder tends to broaden the dispersion peak and close the excitation gap. For a binary distribution, a nondispersing branch at almost zero energy is obtained, in addition to a dispersing branch. We discuss the relationship of our work to the neutron scattering measurement in LiHoF₄.

DOI: [10.1103/PhysRevB.74.172414](https://doi.org/10.1103/PhysRevB.74.172414)

PACS number(s): 75.50.Lk, 05.30.-d, 75.10.Nr, 75.40.Gb

Calculation of real-time dynamics of a correlated quantum system with an infinite number of degrees of freedom are few and far between. Except for isolated examples, construction of real-time behavior from imaginary-time correlation functions (more amenable to numerical methods) by analytic continuation is fraught with various instabilities. The theoretical challenge is particularly acute because neutron scattering experiments often provide a rather detailed map of the frequency, ω , and the wave vector, \mathbf{k} , dependent dynamical structure factor, $S(\mathbf{k}, \omega)$.

The second motivation comes from the desire to study the dynamics of a quantum phase transition involving a zero temperature quantum critical point. In this respect, the Ising spin chain in a transverse field¹⁻⁴ constitutes a schema from which much can be learned about quantum criticality,⁵ both with and without disorder.

The third motivation is to examine how the coherence of the quasiparticle excitations is modified in the presence of quenched disorder and is triggered by a recent neutron scattering experiment⁶ in LiHoF₄, which connects the observed low temperature behavior of $S(\mathbf{k}, \omega)$ in terms of the hyperfine coupling of the electronic spins to a nuclear spin bath, where the Hamiltonian of the electronic spins is given by an Ising model in a transverse field. Because the hyperfine splittings are small, we could imagine that, on the time scale of the electronic motion, this bath will appear essentially quenched, modulating the quantum fluctuations characterized by the transverse field. This is still a bit far from the experimental system, as it is three dimensional, and the Ising couplings are long ranged and dipolar. Nonetheless, we shall see that there are tantalizing similarities between our calculated structure factor and the experimental one in a given direction of the reciprocal space $(2, 0, 0) \rightarrow (1, 0, 0)$ (in reciprocal units). A more appropriate comparison should be with quasi-one-dimensional spin systems that are intentionally disordered.

Finally, the role of disorder in a quantum critical system is an important subject in itself and is certainly not fully understood. In the presence of disorder, there are rare regions with couplings stronger than the average, which results in the Griffiths-McCoy singularities.^{7,8} Although the effect is weak in a classical system, it becomes important in quantum systems, especially in low dimensions.^{9,10}

The Ising model in a random transverse field has been

studied both analytically and numerically,^{9,11-19} and a great number of results of physical importance have been obtained. However, the dynamical structure factor $S(k, \omega)$ has not been computed for all k and ω in the random field model, although some analytical and numerical results are available in pure systems for special values of the wave vector. Here we compute the dynamic structure factor in the presence of two types of disorder distributions: a rectangular and a binary distribution.

The one-dimensional lattice Hamiltonian we study is

$$H = -J \sum_i \sigma_i^z \sigma_{i+1}^z - \sum_i h_i \sigma_i^x, \quad (1)$$

where the σ 's are Pauli matrices, and J is positive and uniform. We shall choose the energy unit such that $J=1.0$. The fields h_i are random variables. The first model we study is the rectangular distribution with a mean h_{ave} and a width h_w . The second model is the binary distribution in which h_i is an independent random variable that takes two values: h_S and h_L with probabilities p and $(1-p)$, respectively. In particular, we choose the parameter p to be small such that the chain is almost spatially homogeneous, $h_S < J < h_L$, to ensure that the system is in the paramagnetic phase. Intuitively, this distribution seems to capture a crude adiabatic representation of the electronic spins coupled to a hyperfine spin bath discussed above, where the larger field is the applied transverse field.

We first compute the time-dependent spin-spin correlation functions $C(n, t) = \overline{\langle \sigma_i^z(t) \sigma_{i+n}^z \rangle}$ at temperature $T=0$, where the angular brackets denote the average over ground state and the overline an average over disorder configurations. The algorithm for evaluating this quantity is similar to that described in Ref. 15, except that we are doing a real time calculation, which entails computation over complex variables. We first perform a Jordan-Wigner transformation²⁰ and then cast the correlation function $C(n, t)$ in the form of a pfaffian, which is calculated efficiently, as described below; after averaging over disorder configurations, the dynamical structure factor is,

$$S(k, \omega) = \sum_n e^{-ikn} \int dt e^{-i\omega t} C(n, t). \quad (2)$$

The pfaffian is the square root of the determinant of an

antisymmetric matrix. Let X be an $N \times N$ (N is even) antisymmetric matrix of the form:

$$X = \begin{bmatrix} A & B \\ -B^T & C \end{bmatrix}, \quad (3)$$

where A is a 2×2 matrix, and B, C are matrices of appropriate dimensions. From the identity:

$$\begin{bmatrix} I_2 & 0 \\ B^T A^{-1} & I_{(N-2)} \end{bmatrix} X \begin{bmatrix} I_2 & -A^{-1}B \\ 0 & I_{(N-2)} \end{bmatrix} = \begin{bmatrix} A & 0 \\ 0 & C + B^T A^{-1}B \end{bmatrix}, \quad (4)$$

where I_n is the unit matrix of dimension n , we have:

$$\text{Det}(X) = \text{Det}(A)\text{Det}(C + B^T A^{-1}B). \quad (5)$$

Since A is also antisymmetric, of the form

$$A = \begin{bmatrix} 0 & a_{12} \\ -a_{12} & 0 \end{bmatrix}, \quad (6)$$

it is easy to invert A , and hence calculate $C + B^T A^{-1}B$. Since the matrix $C + B^T A^{-1}B$ is also antisymmetric of dimension $(N-2)$, the above procedure can be repeated, and the determinant of X is given by the product of 2×2 determinants. Finally, since $\sqrt{\text{Det}(A)} = a_{12}$, the pfaffian of matrix X will be simply a product of $N/2$ numbers obtained from those 2×2 matrices in the above procedure. Because it is not necessary for A to be a 2×2 matrix at the upper left corner of X , for the stability of the algorithm, A is chosen to be a diagonal block such that $|\text{Det}(A)|$ is the largest.

The calculations were performed for a lattice of 160 sites of which 32 sites in the middle were used for evaluating $C(n, t)$. Since we are interested in the gapped phase of the model, where the correlation length is finite, the size of the system was found to be sufficient by checking the difference between the results corresponding to various sizes. A window function, $\exp(-\epsilon_1|t| - \epsilon_2|n|)$, was applied to the Fourier transform in (2) to reduce the cutoff effects in $S(k, \omega)$.¹⁷ The chosen small values $\epsilon_1 = \epsilon_2 = 0.05$ were found to be sufficient for our numerical purposes; the range of the time integration used was $-80 \leq t \leq 80$. Free boundary condition was imposed for simplicity, and the results were averaged over 100 realizations of disorder. We explicitly checked that our conclusions are unaffected in going from say 20 to 100 realizations of disorder. The reason is that we are interested in some robust features of the spectra of excitations in the quantum paramagnetic phase rather than the critical behavior or similar such subtle properties.

To access the paramagnetic regime, in the rectangular distribution case, not too far away from the quantum critical point, we set $h_{ave} = 1.4$. The density of states for Jordan-Wigner fermions is shown in Fig. 1. As we increase disorder, the density of states (DOS) gets broader, and only for strong disorder a few states appear at zero energy, resulting in gapless excitations in this extreme limit. When the disorder width is small, for example $h_w = 0.5$, and the system is still in the paramagnetic regime everywhere, there is only a single dispersing branch, and the excitation remains gapped, as in Fig. 2(a). As we increase h_w , the dynamic structure factor

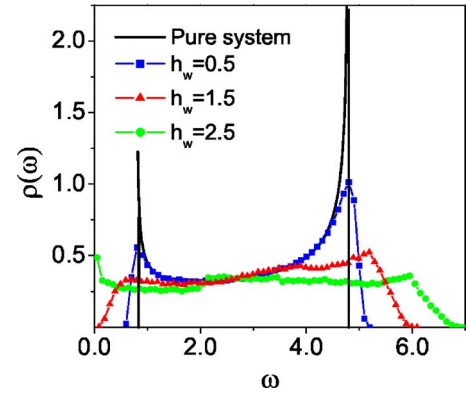


FIG. 1. (Color online) The density of states of Jordan-Wigner fermions, $\rho(\omega)$, for the rectangular distribution, for different disorder strengths. The $\rho(\omega)$ is broadened as h_w increases, and states with gapless excitations are available at zero energy only in the high disorder limit.

can, in principle, have two branches because the DOS can acquire states at zero energy. Clearly, the dispersing branch, as shown in Fig. 2(b), has very low spectral weight everywhere. In principle, there could be a strong nondispersing branch at $\omega=0$. However, since the excitation gap is closed at this value of disorder strength, and since both branches are significantly broadened due to randomness, the nondispersing peak may be mixed with the dispersing branch, and perhaps we are not able to observe them separately. In the high disorder limit, $h_w=2.5$, almost all the intensity concentrates at $(k, \omega) = (0, 0)$, but there appears to be a ghost of the dispersing branch, see Fig. 2(c). An important feature of Figs. 2(b) and 2(c) is the horizontal striplike patterns, which indicate excitation modes that do not disperse, namely the localized modes. Our code was checked by comparing with the exact

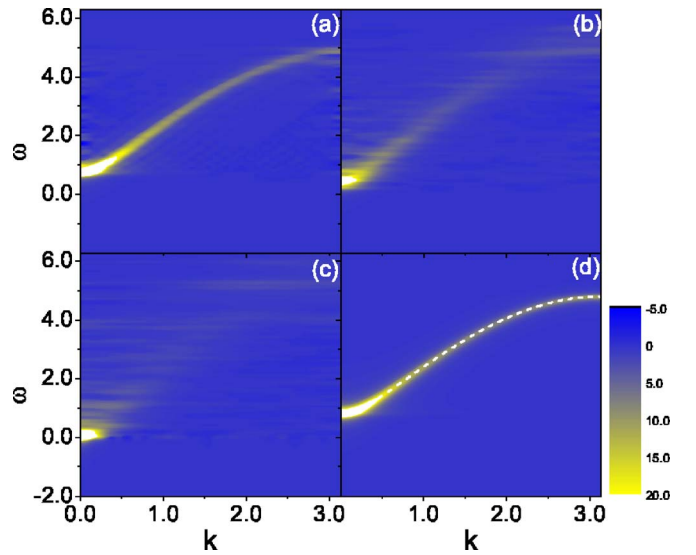


FIG. 2. (Color online) The dynamic structure factor $S(k, \omega)$: (a)–(c) for the rectangular disorder distribution in the paramagnetic phase: $h_{ave} = 1.4$, and $h_w = 0.5, 1.5, 2.5$, respectively; (d) $S(k, \omega)$ for pure system with $h = 1.4$ and $J = 1.0$. Dashed line shows the theoretical dispersion relation.

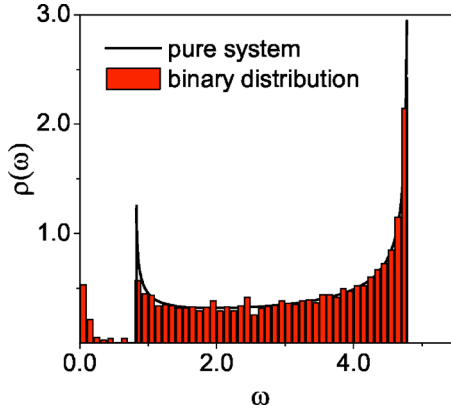


FIG. 3. (Color online) The density of states $\rho(\omega)$ for the binary distribution at $h_L=1.4$. Clearly, a few new states are allowed at zero energy, as the disorder is turned on.

result for the pure system for which $S(k, \omega)$ has a single dispersive branch (see below), though the peak is not a delta function given the finite size of our system; see Fig. 2(d).

In contrast, the binary distribution is quite remarkable. We first choose $h_L=1.4$ so that the system is in the paramagnetic regime, and set $h_S=0.1$, and $p=0.05$. The density of states in Fig. 3 shows zero energy states separated by a gap from the states at higher energy. The calculated $S(k, \omega)$ is shown in Figs. 4(a)–4(f), where $h_L=1.1, 1.2, \dots, 1.6$. While the dispersing branch is broadened due to disorder, the weight of

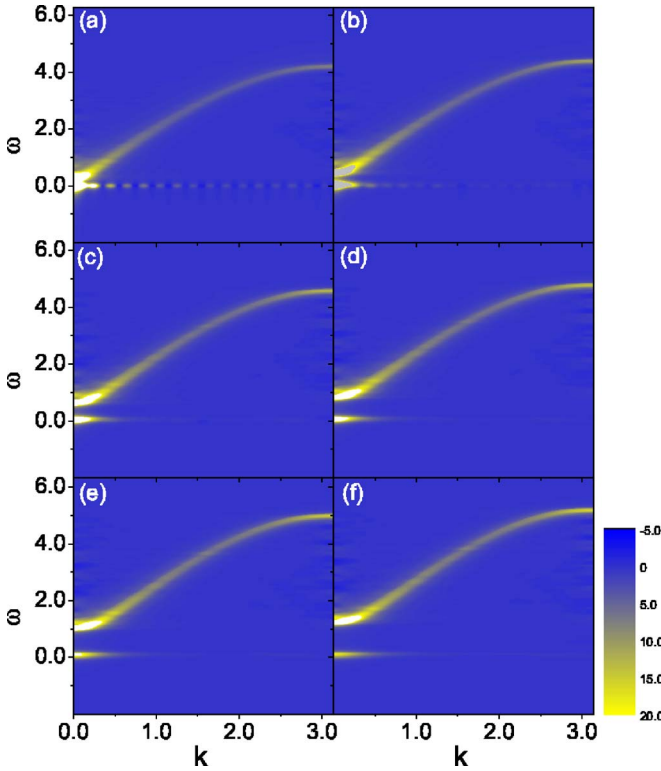


FIG. 4. (Color online) (a)–(f) Dynamic structure factor $S(k, \omega)$ for the binary distribution in the paramagnetic phase. Parameters are $J=1.0$, $h_S=0.1$, $p=0.05$, and $h_L=1.1, 1.2, \dots, 1.6$ from (a) through (f). Both dispersing and nondispersing branches exist, and the excitation is gapped.

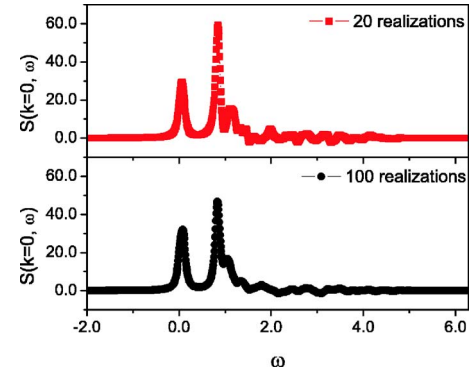


FIG. 5. (Color online) A cut of $S(0, \omega)$ corresponding to Fig. 4(d) for 20 and 100 realizations of disorder.

the central peak around $(k, \omega)=(0, 0)$ is so high that a non-dispersing branch can extend quite far away from the origin.

In Fig. 5, we show a cut of $S(k, \omega)$ at $k=0$, to illustrate that there is hardly any difference between the results averaged over 20 realizations and those averaged over 100 realizations.

Let us define the weight of the central peak as follows:

$$I_h = \frac{\int_{\Delta\Omega} S^2(k, \omega) dk d\omega}{\int_{\Omega} S^2(k, \omega) dk d\omega} \quad (7)$$

where Ω in the denominator is the entire (k, ω) domain, while $\Delta\Omega$ is defined as follows: we first find the maximum of the central peak $S_{\max}(k, \omega)$, and then define the domain $\Delta\Omega$ such that $S(k, \omega) > S_{\max}(k, \omega)/\sqrt{2}$ for $(k, \omega) \in \Delta\Omega$. Note that in (7) we integrate $S^2(k, \omega)$ rather than $S(k, \omega)$. This is because small numerical errors can result in slightly negative values of $S(k, \omega)$ for some (k, ω) , which is obviously unphysical. The dependences of I_h and $\Delta\Omega$ on h_L are plotted in Fig. 6. As we tune h_L from 1.6 to 1.1, I_h increases monotonically, while the region $\Delta\Omega$ shrinks. We conclude that, as the quantum phase transition is approached, the weight is transferred from the dispersing branch to the nondispersing peak.

In addition to the singularity due to the quantum phase transition, in disordered systems there is also the Griffiths-McCoy singularity: the disorder will drive some rare regions into a phase different from the rest. For the pure Ising chain when $h_i=h$, the dispersion relation is (Ref. 2)

$$\omega = 2\sqrt{J^2 + h^2 - 2Jh \cos k}. \quad (8)$$

The excitation gap $\Delta=2|h-J|$ occurs at $k=0$. As $h \rightarrow J$, the excitation gap closes at the quantum critical point. However, if disorder is strong enough, there is nonzero probability to find some regions in which the spins are strongly coupled, such that $h_i < J$ holds, and thus the cluster is ferromagnetic. Calculations, similar to that given in Refs. 5 and 21, show that these clusters give rise to the nondispersing peak at zero energy, as we describe below.

For the binary distribution, the system is almost homogeneous except for the rare regions of strongly coupled clusters

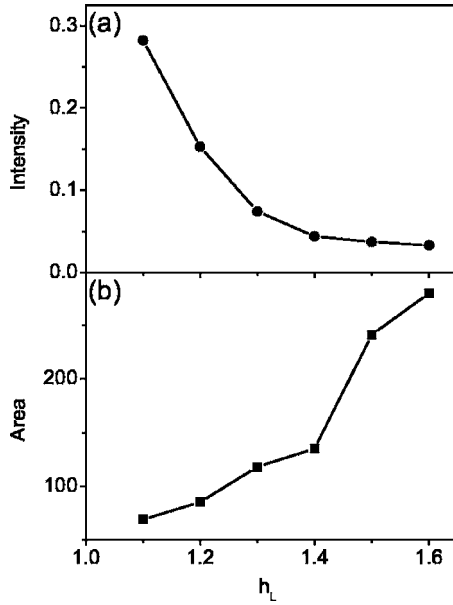


FIG. 6. The binary distribution: as the quantum phase transition is approached from the paramagnetic regime, the central peak intensity I_h increases monotonically, and the area $\Delta\Omega$ corresponding to the half the value of the peak decreases.

where $h_i=h_S$ for all sites inside the cluster. At shorter length scales, the behavior of the pure system dominates, and this leads to the dispersing branch. At longer scales the effects of disorder become important, resulting in the zero energy peak. The autocorrelation function $S(\omega)$, which is the integral of $S(k, \omega)$ over k , can be approximated in the following manner.

The normalized probability that a given site belongs to a ferromagnetic cluster of length L sites is $P(L)=Lp^{L-1}(1-p)^2$. When $h_i=0$ the twofold degenerate ground state within a cluster is far away from the excited states of energy of order $2J$; the perturbation $h_i=h_S$ will split the ground state by $\tilde{g}e^{-cL}$, where \tilde{g} and c are unknown positive constants determined by the details of the Hamiltonian. The form of the splitting results from large order in perturbation theory, however. If we treat these clusters as independent and average over disorder, or equivalently integrate over the cluster size L , we get

$$S(\omega) \sim \int dL P(L) \delta(\omega - \tilde{g}e^{-cL}) \sim \frac{(1-p)^2 \ln(\tilde{g}/\omega)}{p} \frac{\left(\frac{\tilde{g}}{\omega}\right)^{\ln(p)/c}}{\omega}, \quad (9)$$

which diverges at $\omega=0$ if $1 > |\ln p|/c$ modulo logarithmic corrections. We have verified that indeed the divergence disappears for sufficiently small values of p [the peak of $S(\omega)$ is then shifted to ω greater but close to zero, instead], but a detailed verification of this result appears to be difficult.

It is remarkable that a numerically exact solution of a simplified one-dimensional model (binary distribution) can capture some of the experimental features in LiHoF₄ and shed interesting light on the role of disorder on the dynamics of a prototypical quantum critical point. It would be of course interesting to experimentally study intentionally disordered systems that are closer to the model discussed here.

We thank Yifei Lou for suggesting to us the powerful calculational scheme described in the text. This work was supported by the NSF under the Grant No. DMR-0411931.

*Electronic address: sudip@physics.ucla.edu

¹P. G. de Gennes, *Solid State Commun.* **1**, 132 (1963).

²P. Pfeuty, *Ann. Phys. (N.Y.)* **57**, 79 (1970).

³R. J. Elliott, P. Pfeuty, and C. Wood, *Phys. Rev. Lett.* **25**, 443 (1970).

⁴R. B. Stinchcombe, *J. Phys. C* **6**, 2459 (1973).

⁵S. Sachdev, *Quantum Phase Transitions* (Cambridge University Press, Cambridge, 1999).

⁶H. M. Rønnow, R. Parthasarathy, J. Jensen, G. Aeppli, T. F. Rosenbaum, and D. F. McMorrow, *Science* **308**, 389 (2005).

⁷R. B. Griffiths, *Phys. Rev. Lett.* **23**, 17 (1969).

⁸B. M. McCoy, *Phys. Rev. Lett.* **23**, 383 (1969).

⁹D. S. Fisher, *Phys. Rev. B* **51**, 6411 (1995).

¹⁰F. Iglói and C. Monthus, *Phys. Rep.* **412**, 277 (2005).

¹¹B. M. McCoy and T. T. Wu, *The Two-Dimensional Ising Model* (Harvard University Press, Cambridge, 1973).

¹²R. Shankar and G. Murthy, *Phys. Rev. B* **36**, 536 (1987).

¹³A. P. Young and H. Rieger, *Phys. Rev. B* **53**, 8486 (1996).

¹⁴M. Guo, R. N. Bhatt, and D. A. Huse, *Phys. Rev. B* **54**, 3336 (1996).

¹⁵A. P. Young, *Phys. Rev. B* **56**, 11691 (1997).

¹⁶S. Sachdev and A. P. Young, *Phys. Rev. Lett.* **78**, 2220 (1997).

¹⁷O. Derzhko and T. Krokhmal'skii, *Phys. Rev. B* **56**, 11659 (1997).

Different choices of the window functions make little change to our results in accordance with the discussion in W. H. Press, B. P. Flannery, S. A. Teukolsky, and W. T. Vetterling, *Numerical Recipes* (Cambridge University Press, Cambridge, 1986).

¹⁸F. Iglói and H. Rieger, *Phys. Rev. B* **57**, 11404 (1998).

¹⁹C. Pich, A. P. Young, H. Rieger, and N. Kawashima, *Phys. Rev. Lett.* **81**, 5916 (1998).

²⁰E. Lieb, T. Schultz, and D. Mattis, *Ann. Phys. (N.Y.)* **16**, 407 (1961).

²¹See Ref. 5, p. 302.